Available online at www.sciencedirect.com
SCIENCE DIRECT®
Chemistry and Physics of Lipids 122 (2003) 19–32
CPL
CHEMISTRY AND PHYSICS OF LIPIDS
www.elsevier.com/locate/chemphyslip

The peculiar thermo-structural behavior of the anionic lipid DMPG

M. Teresa Lamy-Freund [a,*], Karin A. Riske [b]

[a] *Instituto de Física, Universidade de São Paulo, CP 66 318, CEP 05315-970 São Paulo, SP, Brazil*
[b] *Max Planck Institut of Colloids and Interfaces, Am Mühlenberg 1, 14476 Golm, Germany*

Abstract

Aqueous dispersions of the anionic phospholipid dimyristoyl phosphatidylglycerol (DMPG), around 100 mM ionic strength, are known to exhibit a thermal behavior similar to that of the largely studied lipid dimyristoyl phosphatidylcholine (DMPC), which undergoes a gel to liquid crystalline phase transition at 23 °C, well characterized by differential scanning calorimetry (DSC), and other methods. However, at low ionic strength, DMPG has been shown to present a large gel–fluid transition region, ranging from 18 to 35 °C. This intermediate phase is optically transparent and characterized by a continuous change in membrane packing. Structural properties of the DMPG gel–fluid transition region will be discussed, based on results obtained by several techniques: electron spin resonance (ESR) of spin labels at the membrane surface and intercalated at different depths in the bilayer; light scattering; DSC; small angle X-ray scattering (SAXS); and fluorescence spectroscopy of probes in the bilayer.

Keywords: DMPG; Gel–fluid transition; ESR; Fluorescence; DSC; Light and X-ray scattering

1. Introduction

Under physiological conditions, most cell membranes have a negative charge due to the presence of acidic lipid headgroups. In view of the potential importance of the membrane negative character in many biological processes, anionic phospholipids have been widely used as model systems for possible anionic domains in membranes. Phosphatidylglycerol (PG) is the most abundant anionic phospholipid headgroup present in prokaryotic cell membranes, and has been extensively studied as a model for negatively charged membranes (Seelig et al., 1987; Heimburg and Biltonen, 1994; Biaggi et al., 1997; Fernandez and Lamy-Freund, 2000). Due to the presence of an ionizable phosphate group, the thermo-structural properties of PG-lipids are not only dependent on the hydrocarbon chain length, but also strongly reliant on the pH of the medium and the presence of ions. Dimyristoyl phosphatidylglycerol (DMPG), a saturated lipid with 14-C atoms in each hydrophobic chain, under physiological conditions presents a gel–fluid transition at 23 °C. Hence, it has been considered a rather suitable model system, for instance, for studying peptide–lipid interactions,

* Corresponding author. Tel.: +55-11-3091-6829; fax: +55-11-3813-4334.
E-mail address: mtfreund@if.usp.br (M.T. Lamy-Freund).

0009-3084/02/$ - see front matter
PII: S0009-3084(02)00175-5

as, in the convenient temperature range of 15–40 °C, it would allow to monitor the bilayer in both the gel and fluid phases. The two phases could mimic acidic micro-regions of different fluidity, possibly present in biological membranes at physiological temperatures.

In general, in the study of proteins and peptides that remain at the membrane surface, partially penetrating the bilayer, the electrostatic interaction between their cationic groups and the anionic lipids is essential for increasing their local concentration at the membrane surface. Thus, for studying these systems, it may be necessary to use low ionic strength dispersions, to avoid the decrease in the membrane surface potential due to both counter ions surface binding and shielding, and allow a large protein/peptide concentration at the membrane surface. However, low ionic strength DMPG dispersions were found to present a thermal behavior rather different from that presented by dispersions under physiological conditions. DMPG in the presence of 100 mM NaCl presents a gel–fluid transition profile rather similar to that presented by the zwitterionic lipid dimyristoyl phosphatidylcholine (DMPC), with a sharp differential scanning calorimetry (DSC) peak in the heat capacity profile at 23 °C. However, in a certain range of (low) salt concentration, DMPG displays a different and more complex thermal behavior. The low ionic strength DMPG thermal profile was first studied by Salonen et al. (1989), followed by Heimburg and Biltonen (1994). The first authors showed that DMPG in low ionic strength presented a rather unusual DSC profile, with two distinct peaks in the range of 20–40 °C. They interpreted their data as two phase transitions, identifying the first one with the main gel–fluid transition, T_m, and the second one, not well characterized, was called post-transition, T_{post}. Heimburg and Biltonen (1994) proposed the existence of a gel–fluid transition region between the two main DSC peaks. They observed that, for DMPG in low ionic strength media, there was a correlation between the DSC and the light scattering profiles: there was a sharp decrease in light scattering at the temperature of the first DSC peak, and an increase at the second main DSC peak. They also pointed out that DMPG dispersions were rather viscous in the gel–fluid transition region. Later on, Schneider et al. (1999) proposed the existence of an extended lipid network in the DMPG gel–fluid transition region.

Although the complete characterization of the gel–fluid transition region is far from achieved, the contributions we have made[1] to the better understanding of the thermo-structural behavior of DMPG dispersions will be presented bellow.

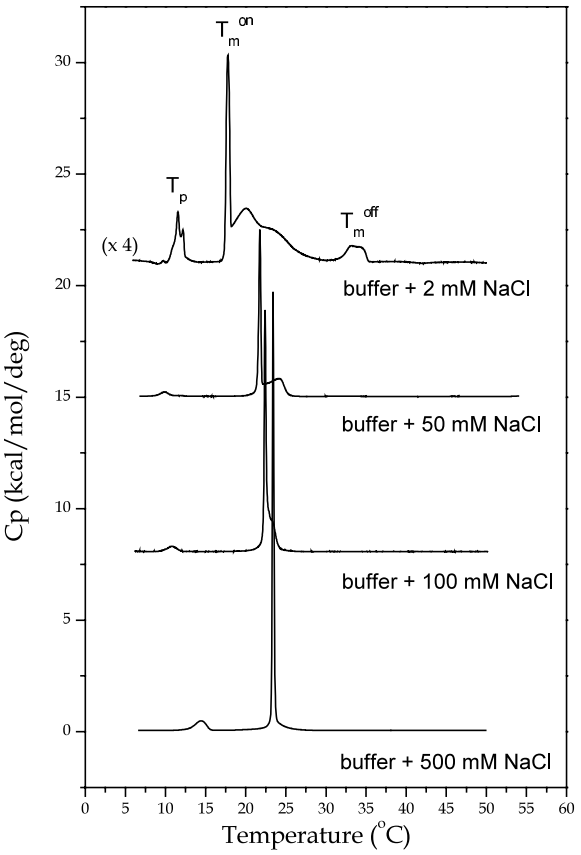

Fig. 1. DSC traces obtained with 10 mM DMPG in buffer (10 mM Hepes pH 7.4) and different NaCl concentrations. For better visualization, the scans were shifted from $C_p = 0$ (adapted from Riske et al., 2002).

[1] M.Phil. and Ph.D. work of K.A. Riske at the Instituto de Fisica, USP-SP, Brazil (Riske et al., 1997, 1999, 2001).

1.1. General properties of DMPG dispersions

As shown in Fig. 1, the DMPG heat capacity (C_p) temperature variation is strongly dependent on the sample ionic strength[2]. Apart from the pre-transition (T_p) at around 12 °C (not the subject of the present work), the low ionic strength DMPG dispersion (in 10 mM Hepes+2 mM NaCl, total ionic strength 6 mM) presents a rather complex calorimetric profile in the range of 17–35 °C, characterized by few broad peaks (Riske et al., 2001). For the reasons discussed bellow, we believe that the melting of the lipid chains starts at the narrow calorimetric peak at T_m^{on} but is only complete at the somewhat broader peak at T_m^{off} (the onset and the offset of the melting regime). This gel–fluid transition region will be called here intermediate phase (between gel and fluid phases). DSC clearly indicates that structural changes are occurring between T_m^{on} and T_m^{off}, evidenced by the presence of broad C_p peaks superimposed in this region. Upon increasing the sample salt concentration, the peaks tend to collapse and the main cooperative peak (T_m) shifts to higher temperature values. This latter effect is related to the known gel phase stabilization due to the screening of the surface charges by counter ions (Träuble et al., 1976).

Table 1 compares the transition molar enthalpies (ΔH) of DMPG in high and low ionic strength and of DMPC. For all three systems, $\Delta H \sim 1$ kcal/mol for the pre-transition. DMPC and DMPG at high ionic strength (100 mM NaCl) present very similar main transition molar enthalpies. It is noteworthy that if the complex calorimetric scan of the low ionic strength DMPG dispersion is integrated for temperatures above 15 °C (including T_m^{on}, T_m^{off} and the region between them), a ΔH value rather similar to those yielded by the main transition of DMPC, or high ionic strength DMPG, is obtained. This strongly suggests that the chain melting of the anionic DMPG bilayers at low ionic strength is spread over a large temperature range (Riske et al., 2001).

The beginning and the end of the DMPG intermediate phase are also characterized by a sharp decrease in turbidity at T_m^{on} and a sharp increase at T_m^{off}, as shown in Fig. 2. Contrary to the turbid gel and fluid phases (below T_m^{on} and above T_m^{off}), the intermediate phase is optically transparent. The light scattering profiles are strongly dependent on the NaCl concentration, as in the DSC traces. A drop in light scattering at T_m, as observed for 100 mM NaCl DMPG sample (Fig. 2), has been attributed to a change in the refractive index increment of the solution per unit mass concentration of lipid (dn/dc), which is related to the known vesicle swelling and corresponding decrease in the bilayer density and thickness at the phase transition (Disalvo, 1991; Yi and MacDonald, 1973). Measurements of n and dn/dc for the low ionic strength sample showed that the variation of these parameters could not explain the large changes in light scattering at T_m^{on} and T_m^{off}, indicating that they must have a different origin (Riske et al., 1997).

The light scattered at different angles by the low ionic strength sample displayed the same pattern as that observed at 90°: between T_m^{on} and T_m^{off} the scattering was significantly less intense than below T_m^{on} and above T_m^{off} (Fig. 3) (Riske et al., 1997). Results from Zimm plots (Zimm, 1948) evidenced a system with considerable polydispersity, detected by the strong scattering at low angles, and only angles from 45° and higher were used in the data analysis (collaboration with M.J. Politi and W.F. Reed; Riske et al., 1997). Though there was significant variation in the results when different preparations were measured, the overall trends were always the same. Below T_m^{on}, the weight average molecular weight of the scatterer (M_w) was higher, and the second virial coefficient (A_2) was very low and negative, indicating some net attraction, and, hence, a possible aggregation of the vesicles. Above T_m^{on}, A_2 becomes positive and large, indicating net repulsion, and M_w drops significantly, while the scatterer z-averaged mean

[2] In the experiments described here, freshly prepared DMPG dispersions were used. A lipid film was formed from a chloroform solution of lipids, dried, and vortexed with the desired concentration of NaCl in 10 mM Hepes buffer solution (4-(2-hydroxyethyl)-1-piperizineethanesulfonic acid) adjusted with NaOH to pH 7.4. For the fluorescence and ESR measurements, the probes were added to the chloroform lipid solution.

Table 1
Transition molar enthalpies, ΔH (kcal/mol), of DMPC and DMPG in high and low ionic strength (n_i)

	T_p	T_m	T_m^{on}	T_m^{off}
DMPC ($n_i = 6$ mM)	0.8±0.2	5.0±0.8		
DMPG ($n_i = 100$ mM)	1.0±0.2	5.7±0.8		
DMPG ($n_i = 6$ mM)	1.0±0.2		1.0±0.2	0.5±0.2
From T_m^{on} to T_m^{off}	5.2±0.8			

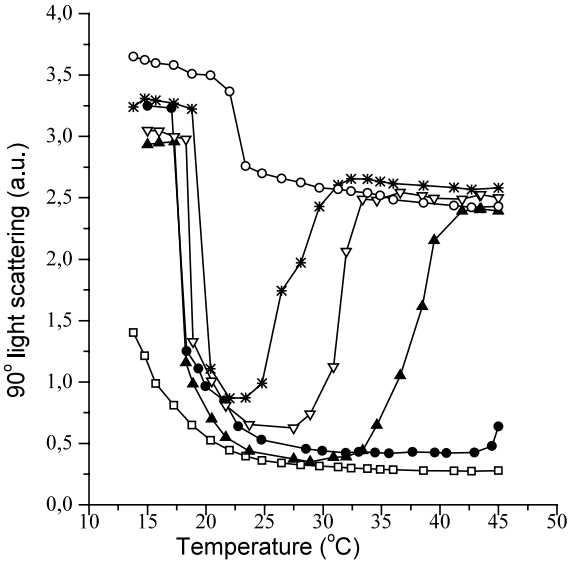

Fig. 2. Temperature dependence of 90° light scattering ($\lambda = 280$ nm) of 10 mM DMPG in different ionic strengths: (□) pure water, (●) Hepes buffer, buffer+(▲) 2 mM, (▽) 5 mM, (*) 10 mM and (○) 100 mM NaCl (Riske et al., 1999).

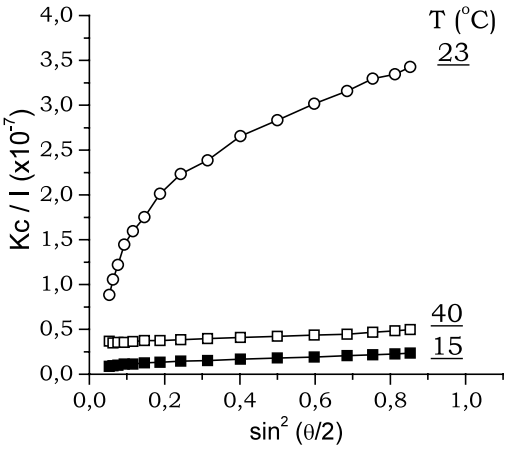

Fig. 3. Kc/I as a function of $\sin^2(\theta/2)$ for 1.0 mM DMPG in Hepes buffer at three temperatures. I is the intensity of light scattered, K is an optical constant, c is the lipid concentration and θ is the scattering angle (Riske et al., 1997).

square radius of gyration $\langle R_g^2 \rangle_z$ increases somewhat. Above T_m^{off} A_2 becomes extremely small or even slightly negative, indicating a considerable decrease in the repulsive force between the vesicles, which parallels an increase in M_w. Apparently, between T_m^{on} and T_m^{off}, a repulsive force between the charged vesicles dominates over the van der Waals attraction. This could be explained by an increase in the vesicle surface charge between T_m^{on} and T_m^{off}, consistent with the observed increase in reduced solution conductivity in this range (Riske et al., 1997). The increase in the bilayer ionization degree α, at T_m^{on}, hence, the increase in the modulus of the electrostatic surface potential, could be related to the dissociation of the sodium ions from the PG headgroups, triggered by the beginning of the gel–fluid transition by some mechanism which has not yet been elucidated.

1.2. DMPG bilayer surface potential (collaboration with O.R. Nascimento, B. Bales and M. Peric)

In an effort to better understand the role of surface electrostatics in the phase transition of DMPG vesicles, a small, highly aqueous soluble, deuterated (to reduce unresolved hyperfine splitting), cationic spin label, 4-trimethylammonium-2,2,6,6-tetramethylpiperidine-d_{17}-1-oxyl iodide (dCAT1), was used to directly monitor the negatively charged DMPG vesicle surface (Riske et al., 1999). Membrane electrostatic surface potential was calculated from the label water/bilayer surface partition ratios, based on a simple two-sites model,

assuming that the electrostatic attraction dominates the interactions between the spin label and DMPG membrane surface. This strategy was based on those used for calculating surface potentials using amphiphilic fluorescent or spin probes, which insert into the bilayer (Castle and Hubbell, 1976; Hartsel and Cafiso, 1986; Khramstov et al., 1992; Franklin et al., 1993; Epand et al., 1996; Krasnowska et al., 1998), but which probe the membrane properties from the 'outside'. Such an approach provides an alternative view and most likely perturbs the membrane less than a probe incorporated into the membrane, apart from yielding ESR signals typical of rapid movement in the ESR timescale, which can be accurately analyzed (Bales, 1989; Marsh, 1989). Moreover, due to the high negative surface potential of DMPG low ionic strength bilayers, an amphiphilic molecule (the same dCAT molecule bound to a 12-C chain, dCAT12) was found to completely partition into the membrane, not allowing the calculation of a surface potential through a water/bilayer partition ratio.

Fig. 4 illustrates how the dCAT1 surface partition ratios (surface label moles/total label moles) could be calculated. The ESR spectrum obtained with dCAT1 in DMPG dispersions (Fig. 4a) was different from that yielded by the label in buffer solution (Fig. 4b), the former clearly indicating the presence of dCAT1 in more than one microenvironment. For most temperatures and ionic strengths, it was possible to decompose the dCAT1 spectrum obtained in DMPG dispersions into two components, one of them corresponding to the label free in solution, here referred as 'free' component. The other component was yielded by labels in a less polar and more packed microenvironment. Fig. 4c shows a typical spectrum obtained after subtracting a weighted free signal (Fig. 4b) from the composite one (Fig. 4a). The weight of the free signal was varied until the resulting spectrum looked like a one component signal and could be well fitted by a Voigt line shape (Bales, 1989). The fact that two well-separated spectra are obtained shows that the exchange rate between the two respective sites is slow on the ESR time scale. In the simple two-site model assumed, the resulting spectrum (Fig. 4c) was yielded by the

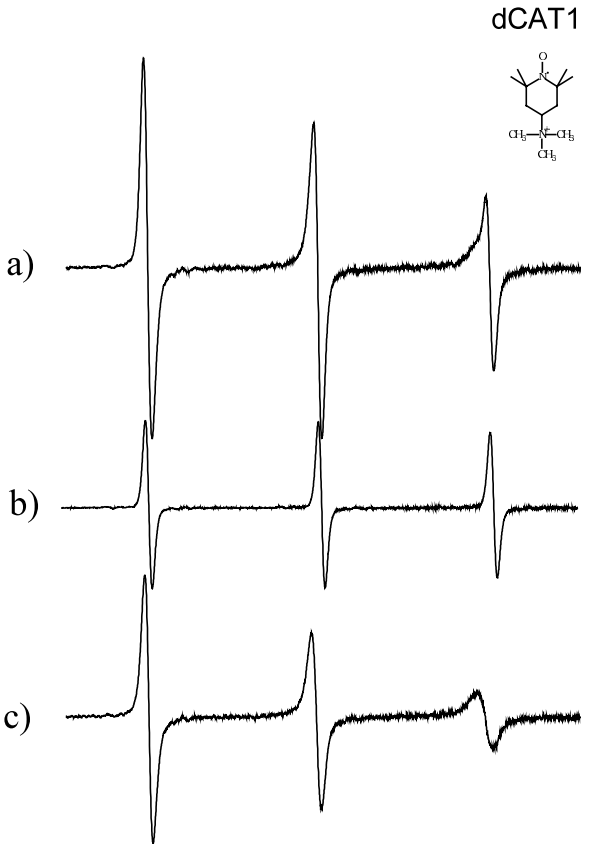

Fig. 4. (a) ESR spectra of 0.1 mM dCAT1 in 10 mM DMPG in Hepes buffer; (b) 0.1 mM dCAT1 free in buffer, (c) a typical ESR spectra subtraction, (a) minus (b). The free (b) and surface (c) components spectra are shown with the real relative intensities that they appear in the composite signal (a). Total spectra width 50 G, $T = 30$ °C (Riske et al., 1999).

population of spin label close to the DMPG surface (an average value), called 'surface dCAT1'.

Decomposition of spectra into free and surface components was carried out for DMPG samples with different ionic strengths at temperatures, between 5 and 45 °C. Membrane surface partition ratios of the probe dCAT1 were calculated from the double integral of the ESR signals (Fig. 5). The values were compared with those obtained with dCAT1 in the 12 mM SDS in water system. The partition ratios calculated for temperatures below 17 °C for DMPG-water, and 20 °C for DMPG-buffer at the various salt concentrations were not very accurate, due to the similarity between the

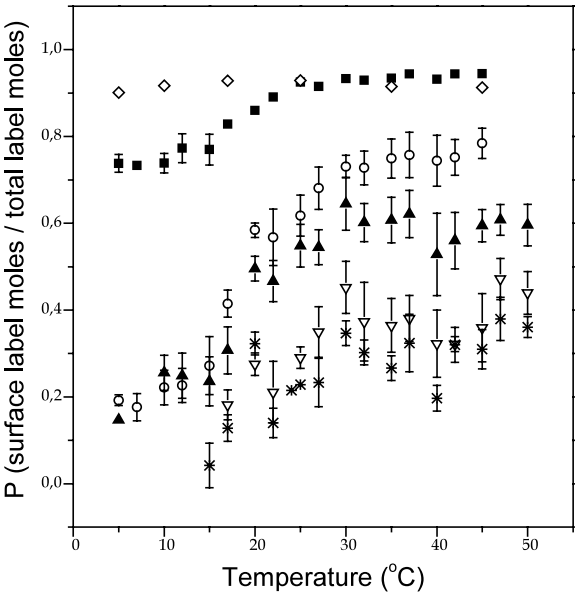

Fig. 5. Partition ratios (surface label moles/total label moles) calculated from the second integral ratio between the surface and the composite spectra. (◇) 12 mM SDS in water, 10 mM DMPG in (■) pure water, (○) Hepes buffer, buffer+(▲) 2 mM, (▽) 5 mM, and (*) 10 mM NaCl (based on Riske et al., 1999).

surface and free components of the ESR spectra (or to the rather small amount of dCAT1 at the bilayer surface), and should be regarded as minimum possible values. Yet, there was a clear tendency of migration of the cationic spin label to the DMPG bilayer surface above T_m^{on}, as compared with the roughly constant value obtained for SDS at all temperatures. That was an indication of an increase in the surface potential at T_m^{on}. Though there were difficulties in the subtractions for temperatures above T_m^{off} (Riske et al., 1999) due to the presence of more than one surface component, as a general rule, the fraction of labels yielding a free ESR signal did not seem to change much for temperatures above T_m^{on}. Therefore, there was no evidence of a decrease in the bilayer surface potential for temperatures above T_m^{off}. The electrostatic character of the force that drives dCAT1 to the DMPG vesicle surface was evidenced by the decrease in dCAT1 membrane partitioning with the increase in ionic strength (Fig. 5). Accordingly, in DMPG-buffer dispersion with 100 mM NaCl, where the PG^- groups are partly shielded by the cations in solution, or in the neutral DMPG in low pH medium (pH 1), the dCAT1 spectra were almost identical to the free spectrum at all temperatures, that is, no surface label could be detected.

Surface electrostatic potential could be only accurately calculated for temperatures above T_m^{on}, namely, for the bilayer in the intermediate or fluid phases. Table 2 shows the calculated potentials for the different ionic strength samples at 30 °C. The values so calculated were compared with those yielded by the Gouy–Chapman–Stern model (see, for instance, McLaughlin, 1977; Evans and Wennerström, 1994). Using a PG^-–H^+ binding constant $K_H = 15.8\ M^{-1}$ (Toko and Yamafuji, 1980; or calculated from Watts et al., 1978), it was found necessary to assume a PG^-–Na^+ binding constant, K_{Na}, different from zero. This is in contrast to the assumption made by some authors that monovalent cations do not bind to PG (Träuble and Eibl, 1974; Träuble et al., 1976; Cevc et al., 1980; Copeland and Andersen, 1982). Allowing for a PG^-–Na^+ binding constant, the Gouy–Chapman–Stern model predicts surface potentials similar to those measured with dCAT1, although the decrease in the surface potential with ionic strength was found to be somewhat steeper than that predicted by the model. The K_{Na} value, estimated between 0.17 and 0.84 M^{-1}, is in the range of the sodium binding constants proposed in the literature (Eisenberg et al., 1979; Loosley-Millman et al., 1982; Lakhdar-Ghazal et al.,

Table 2
DMPG vesicle surface potential (ψ_0) calculated using the partition ratio (P = surface label moles/total label moles) of dCAT1 in lipid suspensions at different ionic strengths (n_i; Riske et al., 1999)

System	n_i (mM)	P	ψ_0 (mV)
DMPG in			
Water	0.1	0.95	−237
Buffer	4.0	0.75	−189
+2 mM NaCl	6.0	0.60	−171
+5 mM NaCl	9.0	0.40	−150
+10 Mm NaCl	14.0	0.25	−132
SDS	0.1	0.90	−220

1983; Helm et al., 1986; Lakhdar-Ghazal and Tocanne, 1988; Tocanne and Tessié, 1990).

1.3. Monitoring DMPG bilayer microenvironments: fluorescent and paramagnetic probes

A gradual decrease in the DMPG membrane packing between T_m^{on} and T_m^{off} was monitored with the fluorescence anisotropy of the probe 1,6-diphenyl-1,3,5-hexatryene (DPH) incorporated into the bilayers. Fig. 6 shows the fluorescence data for low ionic strength DMPG and DMPC membranes. A decrease in fluorescence anisotropy is related to a decrease in acyl chain order, as observed during the gel–fluid transition of lipid membranes. It is evident that the two lipids present similar packing in the gel and fluid phases. However, in contrast to the sharp decrease in the fluorescence anisotropy for DMPC at the gel–fluid transition, DMPG displays a gradual reduction in the bilayer anisotropy from T_m^{on} to T_m^{off}.

It is interesting to point out that, whereas, the relatively large molecule DPH does not monitor any sharp structural transition in the DMPG bilayer, a paramagnetic lipid labeled at the 14th C-atom (1-palmitoyl-2-(14-doxyl stearoyl)-sn-glycero-3-phosphocholine; PCSL), containing the relative small label doxyl, detects a sharp decrease in the membrane packing at T_m^{on}, followed by a continuous decrease till T_m^{off}. Several parameters directly measured from the electron spin resonance (ESR) spectra can quantify chain mobility and/or disorder. We have chosen the ratio of the amplitudes of the central and low field lines (h_0/h_{+1}), due to its sensitivity in monitoring mobility changes and to the accuracy of the measurements

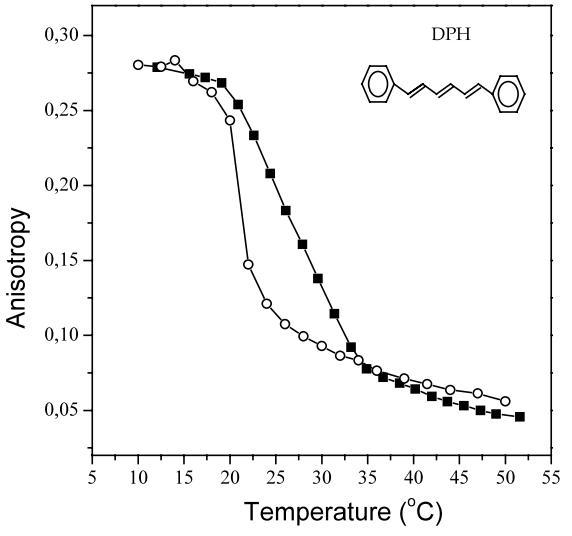

Fig. 6. Fluorescence anisotropy of 0.5 mol% DPH in 1 mM (■) DMPG and (○) DMPC in Hepes buffer+2 mM NaCl (based on Riske et al., 2002).

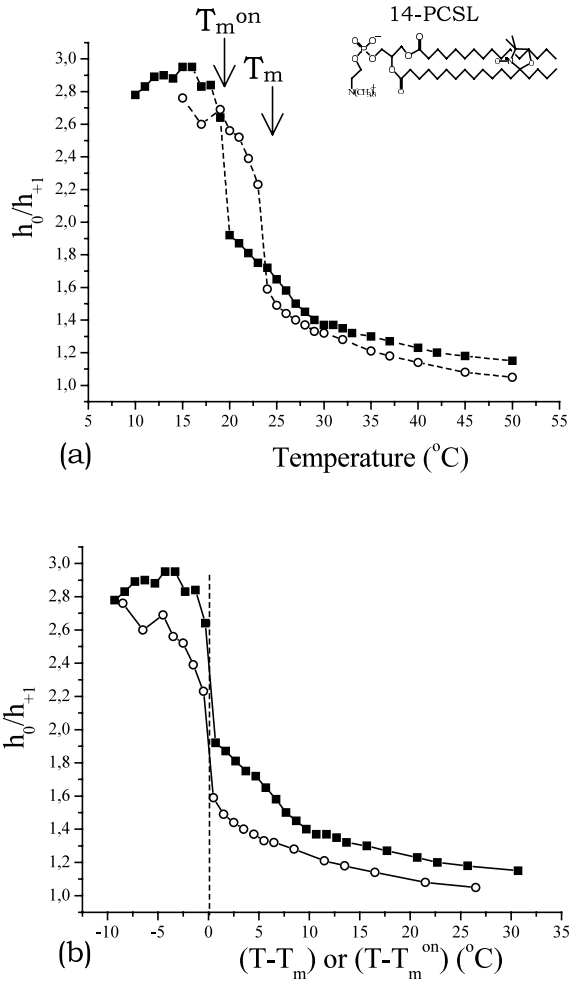

Fig. 7. Temperature dependence of the ratio between the amplitudes of the central and low field resonance lines (h_0/h_{+1}) measured on the ESR spectra of 0.3 mol% 14-PCSL incorporated in (■) 50 mM DMPG in Hepes buffer+2 mM NaCl, and in (○) 10 mM DMPC in buffer (based on Riske et al., 2001).

(Fig. 7). This ratio will decrease tending to unity as the spin label mobility increases. Fig. 7a shows the parameter h_0/h_{+1} measured from the spectra of 14-PCSL incorporated in DMPG and DMPC vesicles, the latter used as a reference. Similar to the results obtained with DPH, the spin label ESR spectra also indicate that the two lipids present similar packing in the gel and fluid phases. For better visualization, the data were also plotted as a function of $(T-T_m^{on})$ for DMPG and $(T-T_m)$ for DMPC (Fig. 7b). It can be clearly seen that there is a great decrease in chain packing of DMPG bilayers at T_m^{on}, followed by a smooth decrease until T_m^{off} is reached. Above T_m^{off} the microviscosity of the fluid phases of DMPC and DMPG are quite similar. On the other hand, DMPC does not show this shoulder, going directly to a fluid phase after T_m. These results are in agreement with those obtained with DSC, and fluorescence anisotropy, indicating that, for low ionic strength DMPG, the melting process is only completed at T_m^{off}. Though less clear, the same behavior is indicated by lipids spin labeled at other positions in the hydrocarbon chain (Riske et al., 1997).

Spin labels also monitor the differences in the gel–fluid transition profile yielded by DMPG dispersions at different ionic strengths, as shown in Fig. 8 for 5- and 12-PCSL (the outer hyperfine splitting A_{max} and the linewidth of the low field line are the empirical parameters used; Riske et al., 1997). It is interesting to point out that the packing of the lipids in the different ionic strength dispersions are very similar for all samples in both the gel (low temperatures) and fluid (high temperatures) phases. Also important, is the information given by the highly anisotropic ESR signal of 5-PCSL (spectra not shown), indicating that DMPG, at all salt concentrations, is organized in bilayers in the whole temperature range studied (for instance, amphiphiles labeled at the 5th C-atom yield a quite different ESR spectrum in micelle-like environment; Benatti et al., 2001).

Very recently, we have found an interesting fingerprint for the DMPG intermediate phase. In this range of temperature, the ESR spectra of phospholipids labeled close to the acyl chain end, at the 16th carbon atom, are likely to be a composition of two signals. One signal is typical

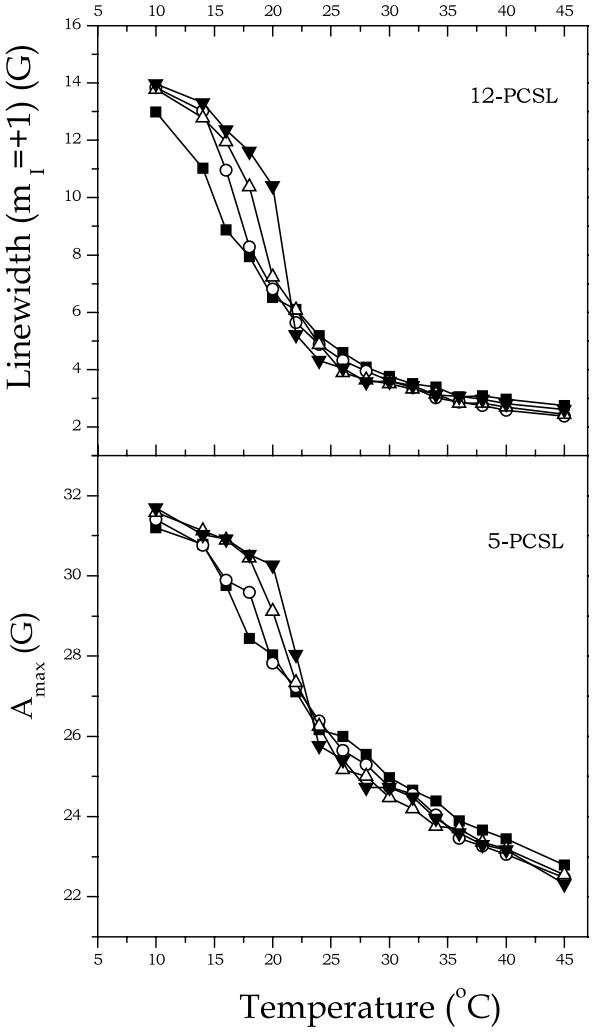

Fig. 8. Measured parameters from ESR spectra of 1 mol% of 12-PCSL and 5-PCSL incorporated in 10 mM DMPG in (■) distilled water, in (○) Hepes buffer, (△) buffer+10 mM and+ (▼) buffer+100 mM NaCl (Riske et al., 1997).

of the nitroxide in a bilayer core (low order, low polarity), and the other one is rather unusual for a bilayer, also corresponding to a low order microenvironment but with a much higher polarity (typical of the 5th C-atom position in a bilayer). Therefore, the experimental results suggest the presence of two structurally different membrane domains in the DMPG intermediate phase (manuscript in preparation). It is important to point out that although the other spin labels (5- to 14-PCSL)

could be partitioned between the two possible different membrane patches, two distinct signals could have been only detected with 16-PCSL due to the faster movement of the nitroxide moiety in this probe, which yields narrower lines in the ESR spectra (Marsh, 1989).

1.4. No membrane fusion

Spin labels were also used to test whether there was vesicle fusion at either T_m^{on} or T_m^{off}. The following experiment was carried out. A phospholipid spin label (16-PCSL), which shows negligible partition into the aqueous medium, incorporated in 10 mM DMPG dispersion was used in a concentration high enough to yield a spectrum broadened by spin exchange (3 mol% of the lipid concentration). One volume of that dispersion was mixed with two volumes of a DMPG sample in the same concentration, but without the spin label. Therefore, if fusion occurred, a significant linewidth decrease would be expected, corresponding to the dilution of the spin label to 1 mol%. No decrease in the spin exchange was observed during and after the following temperature cycle: 30′ at 25 °C, 30′ at 40 °C, 30′ at 17 °C and back to 40 °C. Fig. 9 compares the ESR spectra obtained with 1 and 3 mol% of spin label at 40 °C to evidence the remarkable difference between them. The ESR spectrum obtained after mixing and going through the temperature variations described above (dashed line) is very similar to that obtained for the original sample (3 mol% of label). That experiment indicated that the spin labeled phospholipid could not spread out through the DMPG vesicles added afterwards, which would be expected if fusion had occurred.

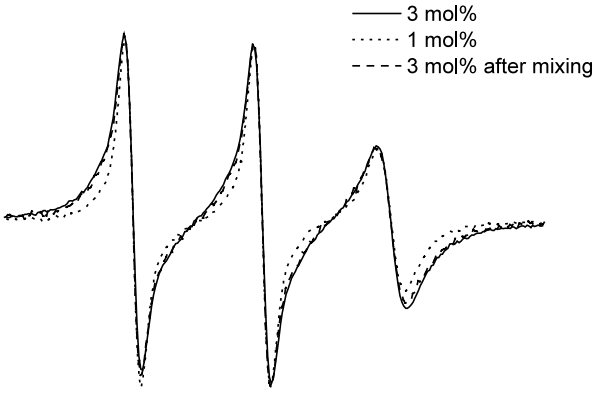

Fig. 9. ESR spectra of 16-PCSL incorporated in DMPG bilayer at (—) 3 and (. . .) 1 mol% of the DMPG concentration, and (---) obtained after mixing samples and going through temperature variations, as described in the text. Total spectra width 80 G, $T = 40$ °C.

1.5. DMPG dispersions monitored by SAXS (collaboration with L.Q. Amaral)

Small angle X-rays scattering (SAXS) has been widely used to characterize the structure of amphiphiles in aqueous media (see, for instance, McIntosh and Simon, 1986; Wiener et al., 1989, 1991; Wiener and White, 1992; Kodama et al., 1997). Many lipids are known to arrange themselves in multibilayer structures with a repeat distance of few nanometers, thus, giving rise to Bragg diffraction in the small angle region. This is illustrated in Fig. 10a for DMPC at various temperatures, indicating a repeat distance of 66 Å in the fluid phase, consistent with previously reported values (Marsh, 1990). The repeat distance corresponds to the bilayer thickness plus the water layer between the lamellae. In contrast to the results obtained with DMPC, low ionic strength DMPG dispersions presented only a broad peak around 0.12 $Å^{-1}$ for the range of lipid concentration (10–50 mM), temperature (10–45 °C) and scattering vector $\mathbf{q}$ (0.03 to 0.35 per Å) studied (Riske et al., 2001), shown in Fig. 10b. Such a broad peak is typical of a single bilayer and arises from the electron density contrast between the bilayer and the solvent (Glatter and Kratky, 1982).

The temperature variation of the peak position ($\mathbf{q}_{max}$) and the maximum intensity (I_{max}) for three different preparations are shown in Fig. 11. In the gel phase the peak was centered at $\mathbf{q}_{max} \approx 0.12$ $Å^{-1}$. Above T_m^{on}, the peak slowly shifted to higher $\mathbf{q}$ values, reaching $\mathbf{q}_{max} \approx 0.13$ $Å^{-1}$ above T_m^{off}. On the other hand, on increasing the temperature the peak intensity started to decrease at T_m^{on} and reached its minimum value just below T_m^{off}, after which the peak intensity increased abruptly. The shift in $\mathbf{q}_{max}$ (associated to a decrease in bilayer thickness) is expected at a gel–fluid transition (McIntosh and Simon, 1986). However, it occurs

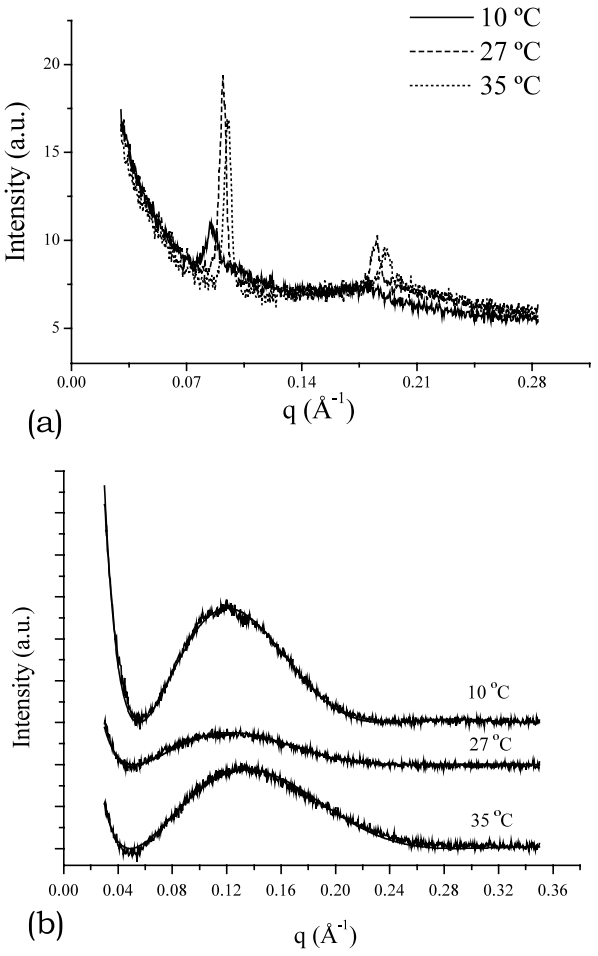

Fig. 10. (a) DMPC in Hepes buffer+2 mM NaCl SAXS curves at 10 °C (below T_m), 27 and 35 °C (above T_m). (b) DMPG in Hepes buffer+2 mM NaCl SAXS curves, and corresponding theoretical fits at 10 °C (below T_m^{on}), 27 °C (between T_m^{on} and T_m^{off}) and 35 °C (above T_m^{off}), for one of the preparations. Curves are shifted for clarity (based on Riske et al., 2001).

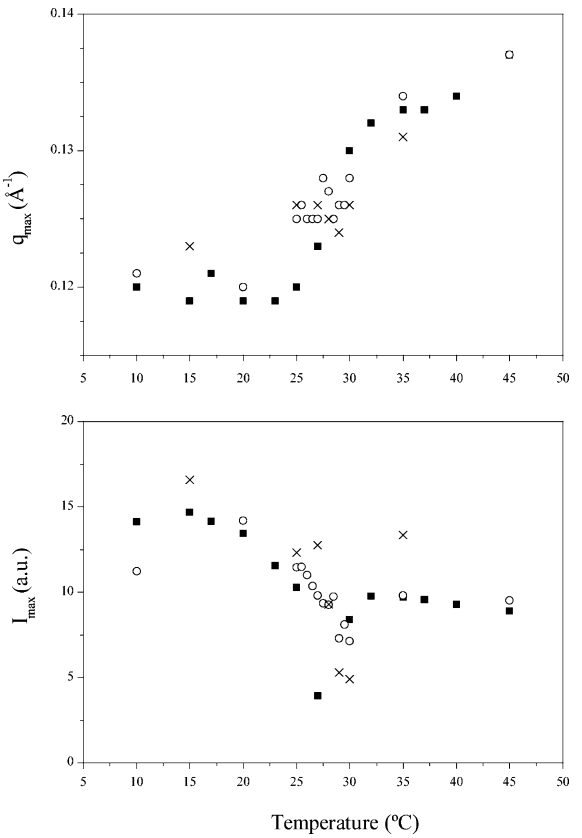

Fig. 11. Temperature dependence of the peak position (top) and maximum intensity (bottom) of the SAXS curves for three different samples (■,○ and ×) of 50 mM DMPG in Hepes buffer+2 mM NaCl. The error in measuring the peak position was estimated to be about 1.5×10^{-3} Å^{-1} and was omitted for a better visualization of the data. The error in the intensity maximum measurement was less than the symbol size (Riske et al., 2001).

sharply at T_m for neutral phospholipids while for DMPG it is spread between T_m^{on} and T_m^{off}. Hence, in agreement with the DSC, fluorescence anisotropy and ESR results, the SAXS data indicate that a complete fluid phase exists only for temperatures above T_m^{off}. The decrease in the X-rays scattering intensity in the melting regime is a remarkable and unusual result.

The SAXS curves (Fig. 10b) can be analyzed using a simple model for the unusual decrease in intensity: a decrease in the bilayer electron density contrast (Riske et al., 2001). The electron density profile $\rho(x)$ of the bilayer is modeled by a three level function, representing the headgroups (ρ_1, R_1), the acyl chains (ρ_2, R_2), and the methyl groups (ρ_3, R_3), and has the meaning of an 'effective profile'. The determination of such $\rho(x)$ does not imply a hypothesis of a single phase in the melting regime. For the understanding of the structural changes involved at T_m^{on} and T_m^{off}, the three SAXS curves showed in Fig. 10b, corresponding to DMPG in the gel, intermediate and

fluid phases were fitted. By using specific constraints to avoid physical inconsistent solutions, the different parameter sets that gave reasonable fit showed only slight changes in their values, always preserving the same trend. The best fits are shown in dashed lines in Fig. 10b and the corresponding $\rho(x)$ functions are presented in Fig. 12.

The main differences between the 10 °C (gel) and 35 °C (fluid) bilayer density profiles are the ones expected to occur between a gel and a fluid phase: the curve at 35 °C was characterized by a clear decrease in the methylene chain thickness as compared with the one found for 10 °C. In the intermediate phase, between T_m^{on} and T_m^{off}, a marked decrease in electron density contrast for the bilayer occurred, both in the headgroup and CH_3 regions. In general, the fits at 27 °C yielded intermediate R_2 values. The electron density contrast in the headgroup region ($\Delta\rho_1$) decreases by almost a factor of two, going from 0.13 at 10 °C to 0.07 at 27 °C. The decrease in electron density absolute values is, however, much smaller (0.46 to 0.40 e/Å^3). Such a decrease could be related to a local increase in the surface area, due to separation between polar headgroups. For a constant R_1, the drop of 13% in ρ_1 corresponds to an increase in headgroup area of the same percentage, meaning that a 6.5% increase in headgroup separation would be enough to explain the drop in intensity. An increase in the methyl group packing at 27 °C is also seen, since R_3 decreases and ρ_3 increases. This could indicate a small degree of interdigitation between the monolayers. The acyl chain density, ρ_2, practically does not change, whereas, R_2 decreases. The abrupt increase in I_{max} at T_m^{off} could correspond to a final rearrangement of the chains in a packed but fluid state, with a decrease in the mean area per headgroup, in view of the increase in ρ_1 observed after T_m^{off} (35 °C in Fig. 12). It is seen, therefore, that the decrease in I_{max} can be explained in terms of reasonable structural changes at the bilayer level. The separation between charged headgroups could also correlate with local fluctuations in membrane curvature and disruptions with water penetration.

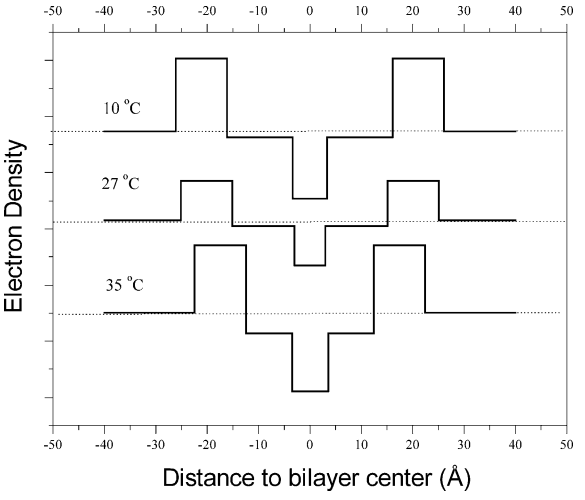

Fig. 12. Bilayer electron density profiles that yielded good fits to the SAXS curves at 10, 27 and 35 °C, are presented in Fig. 10. The profiles are shifted for better visualization. The dotted line represents the bulk aqueous scattering (ρ_w; Riske et al., 2001).

Hence, for DMPG at low ionic strength, apart from the finding that a single bilayer is the basic structure over the whole temperature interval studied, other conclusions emerged from the discussed SAXS analysis: (i) the dominant process seems to be the separation of the charged headgroups, initiated at T_m^{on}, not accompanied by complete melting of the chains, since only a small contraction of the thickness occurs, with some interdigitation at the CH_3 position; (ii) only when the headgroup separation reaches a maximum value, near T_m^{off}, is complete melting achieved and electron density contrast partially recovered.

1.6. Concluding remarks

The presence of an intermediate phase between the gel and fluid phases of freshly prepared DMPG at low ionic strength is well established. This phase appears over a wide lipid concentration range (at least 1–50 mM; Riske et al., 2002) under conditions at which the DMPG surface potential is high: pH values above 6 and salt concentration below 100 mM. Fluorescent and spin probes tell us that for temperatures bellow T_m^{on} the DMPG bilayer is highly packed, in a gel phase, and above T_m^{off} the bilayer is fluid. The packing of the gel and

fluid phases is similar for DMPG at all ionic strengths studied (from pure water to 100 mM NaCl) and similar to that of DMPC. At T_m^{on} there is a sharp decrease in membrane packing (monitored by spin labels only), followed by a gradual increase in the membrane fluidity till T_m^{off}. Therefore, the intermediate phase is a gel–fluid transition region, over which the melting of the acyl chains occurs. This is also confirmed by the presence of several calorimetric peaks in the DSC profile between T_m^{on} and T_m^{off}. On the other hand, the intermediate phase clearly has specific properties, such as very low turbidity and high viscosity (Heimburg and Biltonen, 1994) and electrical conductivity (Riske et al., 1997), and is delimited by defined calorimetric peaks at T_m^{on} and T_m^{off}. The existence of the intermediate phase was shown to be strictly related to the presence of negative phosphate groups at the DMPG surface, since by increasing the salt and/or proton concentrations the intermediate phase vanishes (Riske et al., 2002), and a highly cooperative gel–fluid transition occurs, similar to ubiquitous PC-lipids.

Even though the existence of the intermediate phase is well accepted, its structural characteristics are still the subject of controversy. One hypothesis, raised by Schneider et al. (1999), proposes that this intermediate phase consists of an extended three-dimensional bilayer network. However, the fact that no vesicle fusion, necessary for the formation of an extended lipid network, was observed at any temperature, do not support this hypothesis. Other proposed model (Goldman et al., 1999; Goldman, 2001), a statistical approach considering surface fluctuations, also assumes lipids redistribution.

The results obtained so far could be rationalized considering that, in low ionic strength DMPG bilayers, the lipid gel–fluid transition does not occur abruptly, but there is a competition among the different temperature dependent lipid–lipid interactions. At T_m^{on} a Na^+–PG^- dissociation process would be triggered by some mechanism still not understood, increasing the membrane surface potential, with correlated changes in viscosity and light scattering. Thus, a strong repulsion between adjacent headgroups would start the melting regime, monitored as a sharp event in DSC and ESR of spin labels. From T_m^{on} onward there would be a competition among different interactions, namely headgroup repulsion, van der Waals inter-chain attraction and intra-bilayer repulsion between monolayers, resulting in a large gel–fluid temperature region. This could bring a coexistence of domains with different packing characteristics, which could explain the gradual variation of the several parameters measured with the different techniques described here, over the temperature interval T_m^{on}–T_m^{off}. This would certainly induce membrane deformations imposed by the coexistence of more rigid and flat patches with softer and highly curved regions, similar to morphological observations of giant vesicles at the main phase transition (over a much narrower temperature interval though; Sackmann, 1995; Bagatolli and Gratton, 1999). At T_m^{off}, marked by a broad calorimetric peak, there would be a rearrangement of the lipid packing bringing the membrane to a homogeneous fluid phase.

It is interesting to point out that DSC traces indicated that, whereas, the saturated PG lipid with 12-C chains (DLPG) presented an intermediate phase over an even larger temperature interval than that of DMPG, the longer chain lipid DPPG (16-C) displayed a sharp DSC peak (Schneider et al., 1999), typical of a highly cooperative gel–fluid transition. That confirms the critical role played by the different lipid–lipid interactions in the existence of the gel–fluid transition region: different chainlengths would alter the balance among the different interactions.

Though much has been found about the DMPG intermediate phase, a comprehensive explanation of the anomalous behavior of low ionic strength PG lipids is still necessary. That would contribute to the better understanding of the interesting physicochemical problem concerning the interactions present in a charged aqueous lipid dispersion, both inter and intra bilayers.

Acknowledgements

The authors would like to thank all their collaborators in the works cited here. The work was supported by USP, FAPESP, CNPq, and CAPES/DAAD.

References

Bagatolli, L.A., Gratton, E., 1999. Two-phase fluorescence microscopy observation of shape changes at the phase transition in phospholopid giant unilamellar vesicles. Bipohys. J. 77, 2090–2101.

Bales, B.L., 1989. Inhomogeneously broadened spin-label spectra. In: Berliner, L.J., Reuben, J. (Eds.), Biological Magnetic Resonance, vol. 8. Plenum Publishing Corporation, New York, pp. 77–129.

Benatti, C.R., Feitosa, E., Fernandez, R.M., Lamy-Freund, M.T., 2001. Structural and thermal characterization of dioctadecyldimethylammonium bromide dispersions by spins labels. Chem. Phys. Lipids 111, 93–104.

Biaggi, M.H., Riske, K.A., Lamy-Freund, M.T., 1997. Melanotropic peptides–lipid bilayer interaction. Comparison of the hormone α-MSH to a biologically more potent analog. Biophys. Chem. 67, 139–149.

Castle, J.D., Hubbell, W.L., 1976. Estimation of membrane surface potential and charge density from the phase equilibrium of a paramagnetic amphiphile. Biochemistry 15, 4818–4831.

Cevc, G., Watts, A., Marsh, D., 1980. Non-electrostatic contribution to the titration of the ordered-fluid phase transition of phosphatidylglycerol bilayers. FEBS Lett. 120, 267–270.

Copeland, B.R., Andersen, H.C., 1982. A theory of effects of protons and divalent cations on phase equilibria in charged bilayer membranes: comparison with experiments. Biochemistry 21, 2811–2820.

Disalvo, E.A., 1991. Optical properties of lipid dispersions induced by permeant molecules. Chem. Phys. Lipids 59, 199–206.

Eisenberg, M., Gresalfi, T., Riccio, T., McLaughlin, S., 1979. Adsorption of monovalent cations to bilayer membranes containing negative phospholipids. Biochemistry 18, 5213–5223.

Epand, R.F., Kraayenhof, R., Sterk, G.J., Sang, H.W.W.F., Epand, R.M., 1996. Fluorescent probes of membrane surface properties. Biochim. Biophys. Acta 1284, 191–195.

Evans, D.F., Wennerstöm, H., 1994. Electrostatic interactions in colloidal systems. In: The Colloidal Domain, Where Physics, Chemistry, Biology, and Technology Meet. VCH Publishers, New York, pp. 110–114.

Fernandez, R.M., Lamy-Freund, M.T., 2000. Correlation between the effects of a cationic peptide on the hydration and fluidity of anionic lipid bilayers: a comparative study with sodium ions and cholesterol. Biophys. Chem. 87, 87–102.

Franklin, J.C., Cafiso, D.S., Flewelling, R.F., Hubbell, W.L., 1993. Probes of membrane electrostatics: synthesis and voltage-dependent partitioning of negative hydrophobic ion spin labels in lipid vesicles. Biophys. J. 64, 642–653.

Glatter, O., Kratky, O., 1982. Small Angle X-Ray Scattering. Academic Press, New York.

Goldman, C., 2001. Modified surface fluctuations by impurity binding in amphiphilic dispersions. J. Chem. Phys. 114, 6242–6248.

Goldman, C., Riske, K.A., Lamy-Freund, M.T., 1999. Role of soft and hard aggregates in the thermodynamics of lipid dispersions. Phys. Rev. E60, 7349–7353.

Hartsel, S.C., Cafiso, D.S., 1986. Test of discreteness-of-charge effects in phospholipid vesicles: measurements using paramagnetic amphiphiles. Biochemistry 25, 8214–8219.

Heimburg, T., Biltonen, R.L., 1994. Thermotropic behavior of dimyristoylphosphatidylglycerol and its interaction with cytochrome *c*. Biochemistry 33, 9477–9488.

Helm, C.A., Laxhuber, L., Lösche, M., Möhwald, H., 1986. Electrostatic interactions in phospholipids membranes. I: Influence of monovalent ions. Colloid. Polym. Sci. 264, 46–55.

Khramstov, V.V., Marsh, D., Weiner, L., Reznikov, V.A., 1992. The application of pH-sensitive spin labels to studies of surface potential and polarity of phospholipid membranes and proteins. Biochim. Biophys. Acta 1104, 317–324.

Kodama, M., Aoji, H., Takahashi, H., Hatta, I., 1997. Interlamellar waters in dimyristoylphosphatidylethalonamine–water system as studied by calorimetric and X-ray diffraction. Biochim. Biophys. Acta 1329, 61–73.

Krasnowska, E.K., Gratton, E., Parasassi, T., 1998. Prodan as a membrane surface fluorescence probe: partitioning between water and phospholipid phases. Biophys. J. 74, 1984–1993.

Lakhdar-Ghazal, F., Tocanne, J.F., 1988. Modulation of the adsorption of alkaline cations to phosphatidylglicerol by a dimannosyldiacylglycerol. Biochim. Biophys. Acta 943, 19–27.

Lakhdar-Ghazal, F., Tichiadou, J.L., Tocanne, J.F., 1983. Effect of pH and monovalent cations on the ionization state of phosphatidylglycerol in monolayers. Eur. J. Biochem. 134, 531–537.

Loosley-Millman, M.E., Rand, R.P., Parsegian, V.A., 1982. Effects of monovalent ion binding and screening on measured electrostatic forces between charged phospholipid bilayers. Biophys. J. 40, 221–232.

Marsh, D., 1989. Experimental methods in spin-label spectral analysis. In: Berliner, L.J., e Reuben, J. (Eds.), Biological Magnetic Resonance, vol. 8. Plenum Publishing Corporation, New York, pp. 255–303.

Marsh, D., 1990. CRC Handbook of Lipid Bilayers. CRC Press, Boca Raton.

McIntosh, T.J., Simon, S.A., 1986. Area per molecule and distribution of water in fully hydrated dilaurylphosphatidylethalonamine bilayers. Biochemistry 25, 4948–4952.

McLaughlin, S., 1977. Electrostatic potentials at membrane–solution interfaces. Curr. Top. Membr. Transp. 9, 71–144.

Riske, K.A., Politi, M.J., Reed, W.F., Lamy-Freund, M.T., 1997. Temperature and ionic strength dependent light scattering of DMPG dispersions. Chem. Phys. Lipids 89, 31–44.

Riske, K.A., Nascimento, O.R., Peric, M., Bales, B., Lamy-Freund, M.T., 1999. Probing DMPG vesicle surface with a cationic aqueous soluble spin label. Biochim. Biophys. Acta 1418, 133–146.

Riske, K.A., Amaral, L.Q., Lamy-Freund, M.T., 2001. Thermal transitions of DMPG bilayers in aqueous solution: SAXS structural studies. Biochim. Biophys. Acta 1511, 297–308.

Riske, K.A., Döbereiner, H.-G., Lamy-Freund, M.T., 2002. Gel-fluid transition in dilute versus concentrated DMPG aqueous dispersions. J. Phys. Chem. B 106, 239–246.

Sackmann, E., 1995. Physical basis of self-organization and function of membranes: physics of vesicles. In: Lipowsky, R., Sackmann, E. (Eds.), Structure and Dynamics of Membranes. From Cells to Vesicles. Elsevier/North Holland, Amsterdam, pp. 213–304.

Salonen, I.S., Eklund, K.K., Virtanen, J.A., Kinnunen, P.K.J., 1989. Comparison of the effects of NaCl on the thermotropic behaviour of *sn*-1′ and *sn*-3′ stereoisomers of 1,2-dimyristoyl-*sn*-glycero-3-phosphatidylglycerol. Biochim. Biophys. Acta 982, 205–215.

Schneider, M., Marsh, D., Jahn, W., Kloesgen, B., Heimburg, T., 1999. Network formation of lipid membranes: triggering structural transitions by chain melting. Proc. Natl. Acad. Sci. USA 96, 14312–14317.

Seelig, J., MacDonald, P.M., Scherer, P.G., 1987. Phospholipid head groups as sensors of electric charge in membranes. Biochemistry 26, 7535–7541.

Tocanne, J.F., Tessié, J., 1990. Ionization of phospholipids and phospholipid-supported interfacial lateral diffusion of protons in membrane model systems. Biochim. Biophys. Acta 1031, 111–142.

Toko, K., Yamafuji, K., 1980. Influence of monovalent and divalent cations on the surface area of phosphatidylglycerol monolayers. Chem. Phys. Lipids 26, 79–99.

Träuble, H., Eibl, H., 1974. Electrostatic effects on lipid phase transitions: membrane structure and ionic environment. Proc. Natl. Acad. Sci. USA 71, 214–219.

Träuble, H., Teubner, M., Wooley, P., Eibl, H., 1976. Electrostatic interactions at charged lipid membranes. I. Effects of pH and univalent cations on membrane structure. Biophys. Chem. 4, 319–342.

Watts, A., Harlos, K., Maschke, W., Marsh, D., 1978. Control of the structure and fluidity of phosphatidylglycerol bilayers by pH titration. Biochim. Biophys. Acta 510, 63–74.

Wiener, M.C., White, S.H., 1992. Structure of a fluid dioleoyl phosphatidylcholine bilayer determined by joint refinement of X-ray and neutron diffraction data. III. Complete structure. Biophys. J. 61, 434–447.

Wiener, M.C., Suter, R.M., Nagle, J.F., 1989. Structure of the fully hydrated gel phase of dipalmitoylphosphatidylcholine. Biophys. J. 55, 315–325.

Wiener, M.C., King, G.I., White, S.H., 1991. Structure of a fluid dioleoylphosphatidylcholine bilayer determined by joint refinement of X-ray and neutron diffraction data. I. Scaling of neutron data and the distribution of double bonds and water. Biophys. J. 60, 568–576.

Yi, P.N., MacDonald, R.C., 1973. Temperature dependence of optical properties of aqueous dispersions of phosphatidylcholine. Chem. Phys. Lipids 11, 114–134.

Zimm, B.H., 1948. The scattering of light and the radial distribution function of high polymer solutions. J. Chem. Phys. 16, 1093–1116.